

# Estimation of the storage life of dimethylol urea using non-isothermal accelerated testing

T. Fukumoto · P. S. Thomas · B. H. Stuart ·  
P. Simon · G. Adam · R. Shimmon ·  
J.-P. Guerbois

3<sup>rd</sup> Joint Czech-Hungarian-Polish-Slovak Thermoanalytical Conference Special Chapter  
© Akadémiai Kiadó, Budapest, Hungary 2011

**Abstract** The mechanism and stability of dimethylol urea (DMU) to polycondensation were investigated using thermogravimetric analysis coupled with mass spectroscopy (TG-MS) for evolved gas analysis and a non-isothermal model-free induction period kinetic analysis using three temperature functions; the Arrhenius function and two non-Arrhenian functions. The polycondensation was observed to occur through a two-step process of condensation followed by elimination of formaldehyde during structural rearrangement as has been reported in the literature. The rate equations for each temperature function were evaluated and extrapolated to room (23 °C) and refrigerator (4 °C) temperature to estimate the length of the induction period for the onset of polycondensation for storage life prediction. Based on experience, estimates of the length of the induction periods and, hence, storage life, were most realistically predicted by the non-Arrhenian temperature functions.

**Keywords** Dimethylol urea · Polycondensation · Induction period · Non-isothermal kinetics · TG

## Introduction

Dimethylol urea (DMU) has been extensively utilised as a finishing additive for the cross-linking of cellulose fibres [1], as an ingredient in disinfectant and cleansing fluid, and as a preservative for cooling lubricants [2]. It is generally agreed that the reaction of urea with formaldehyde results in the synthesis of methylol urea via a methylation reaction [3, 4] and that 1 mol of urea reacts with 2 mol of formaldehyde to produce DMU (Fig. 1) [5]. DMU, however, is susceptible to polymerisation through subsequent condensation reactions that form a polycondensate [3, 4, 6]. The loss of water during the condensation reaction leads to the formation of unstable methylene-ether ( $-\text{CH}_2-\text{O}-\text{CH}_2-$ ) bridges from which formaldehyde is eliminated when methylene-ether bridges are rearranged to form methylene ( $-\text{CH}_2-$ ) bridges (Fig. 1) [4, 7].

Owing to its tendency to polymerise during long-term storage, an accurate estimation of DMU's storage lifetime is important. The storage lifetime can be estimated using a model-free kinetic analysis of the length of the induction period (defined as the onset of polycondensation) using non-isothermal methods [8, 9]. Typically, the kinetic analysis is made using an Arrhenius temperature function resulting in the improper integral:

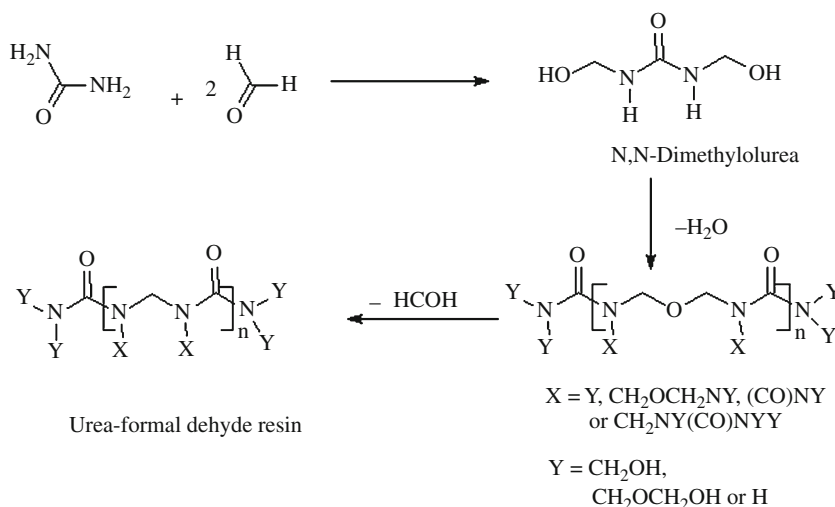
$$\beta = \int_0^{T_i} \frac{dT}{A \exp(B/T)} \quad (1)$$

where  $A$  and  $B$  are the kinetic parameters and  $T_i$  is temperature at the end of the induction period measured under non-isothermal conditions using a linear heating rate ( $\beta$ ) [8]. In order to determine the kinetic parameters  $A$  and  $B$ , Eq. 1 must be integrated using an iterative method

T. Fukumoto · P. S. Thomas (✉) · B. H. Stuart · G. Adam ·  
R. Shimmon · J.-P. Guerbois  
School of Chemistry and Forensic Science, University of  
Technology Sydney, PO Box 123, Sydney, NSW 2007, Australia  
e-mail: paul.thomas@uts.edu.au

P. Simon  
Institute of Physical Chemistry and Chemical Physics, Faculty of  
Chemical and Food Technology, Slovak University of  
Technology, Radlinského 9, 812 37 Bratislava, Slovak Republic

**Fig. 1** The reaction scheme for the formation of urea-formaldehyde resins



which, for the current paper, is carried out using a program based on the Simpson method that was devised for calculating the induction periods for the vulcanisation of rubber [8] and recrystallisation of nickel(II) sulphide [10]. Once the kinetic parameters have been determined the length of the isothermal induction period,  $t_i$ , at any temperature can be calculated from:

$$t_i = A \exp\left(\frac{B}{T}\right) \quad (2)$$

The processes involved in determining the length of the induction period are likely to be complex and must occur even though they are unknown, unobservable and undefined. As these processes may not necessarily conform to an activated state type mechanism, alternative temperature functions may be applied to the kinetic analysis [11]. In this paper, two such functions, which relate the temperature at the end of the induction period,  $T_i$ , to the heating rate,  $\beta$ , in non-isothermal measurements, are applied [9, 12]:

$$T_i = \frac{1}{D} \ln(CD\beta + 1) \quad (3)$$

where  $C$  and  $D$  are adjustable parameters, and

$$T_i = T_\infty(1 - \exp(-\beta^a)) \quad (4)$$

where  $T_\infty$  is the temperature the end of the induction period for an infinite heating rate and  $a$  is an exponent. Once the kinetic parameters of Eqs. 3 and 4 have been determined, the length of the induction period at any temperature under isothermal conditions may be estimated from:

$$t_i = C \exp(-DT) \quad (5)$$

and

$$t_i = (T_\infty - T)a \left( \ln \frac{T_\infty}{(T_\infty - T)} \right)^{\frac{a-1}{a}}, \quad (6)$$

respectively. The advantage of using Eqs. 3 and 4 for the determination of the kinetic parameters is that manipulation of these functions is simpler than in the case of Eq. 1.

For this study, thermogravimetric analysis (TG) was used to measure the end of the induction period as a function of heating rate and Eqs. 1, 3 and 4 were used to model the kinetics of the reaction. Values for the kinetic parameters determined were then used to estimate the length of the induction period at laboratory temperature (23 °C) and refrigerator temperature (4 °C) using Eqs. 2, 5 and 6 and, hence, the storage life was estimated. In order to ensure that the measured onset temperatures used to determine the end of the induction period corresponded to the polycondensation as described in Fig. 1, evolved gas analysis (thermogravimetric analysis coupled with mass spectroscopy (TG-MS)) was used to identify evolved products associated with the initial mass loss step.

## Experimental methods

### Materials

To synthesise DMU, urea (>99%, BDH, Australia) and an aqueous formalin solution (34–40%, AJAX Chemicals, Australia) as a source of formaldehyde were used as starting materials. The aqueous NaOH solutions were prepared from NaOH pellets (97%, Ajax Finechem, Australia).

### Synthesis of DMU

DMU was synthesised according to a method described in the literature [13]. A sodium phosphate buffer with pH 8 was prepared by mixing 47.35 mL of a 0.2 mol/L disodium hydrogen orthophosphate solution and 2.65 mL of 0.2 mol/L

L sodium dihydrogen phosphate. Urea and formalin solution at a molar ratio of 1:2.5 were mixed in an Erlenmeyer flask on a magnetic stirrer. After the pH of the solution was adjusted to 8–9 by the dropwise addition of 10% w/v NaOH solution, the resulting solution was buffered with a few drops of sodium phosphate buffer solution at pH 8 and was stirred at room temperature for 15 h with a magnetic stirrer. The white precipitate was filtered with a Büchner funnel and then washed with three 5 mL portions of 10% v/v ethanol solution. To remove traces of moisture and formaldehyde, the precipitates were immersed in liquid nitrogen and dried in a freeze-dryer (Martin Christ Alpha 2–4 LD plus) overnight. Confirmation of the product was obtained by comparison of the  $^1\text{H}$ ,  $^{13}\text{C}$  NMR spectra, IR and the melting point with those reported in the literature [4, 14].

### Thermogravimetric analysis

TG was carried out using a TA Instruments SDT 2960 simultaneous DTA-TG analyser. Samples of DMU (5–7 mg) were heated from 35 to 400 °C at heating rates of 0.5, 1, 2, 5 and 10 °C min<sup>-1</sup>. All measurements were performed in air with a flow rate of 20 mL min<sup>-1</sup>. The TG-MS measurements were carried out using a Setaram Setsys 16/18 thermoanalyser coupled to a Balzers ThermoStar quadrupole mass spectrometer. Samples were heated from room temperature to 400 °C at a heating rate of 5 °C min<sup>-1</sup> in a flowing argon atmosphere.

### Results and discussion

The TG-MS data are shown in Fig. 2, within which the DTG data is compared to a range of MS peaks. Three DTG peaks are observed in this range centred on 117, 215 and 288 °C. The initial peak at 117 °C correlates with the evolution of water (18 amu) and formaldehyde (29 and 30 amu) suggesting that the polycondensation of DMU is occurring at this temperature in accordance with the scheme laid out in Fig. 1. The higher temperature steps also result in the evolution of water and formaldehyde and significant proportions of carbon dioxide (44 amu) indicating that the decomposition of the polymerised DMU is occurring. This is confirmed by the presence of peaks in the 15 amu curve which represents N–H<sup>+</sup> species. The degradation process increases in its complexity as the temperature is raised where upon gas phase reactions producing NO are observed in the 30 amu curve above 350 °C.

Although the initial mechanism of polymerisation of the DMU corresponds with the polycondensation described by Fig. 1, the mechanism quickly changes and, thus, a

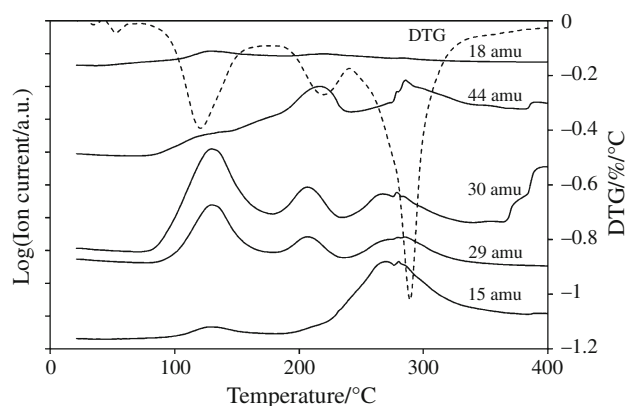


**Fig. 2** DTG and MS data for the polymerisation of DMU at a heating rate of 5 °C min<sup>-1</sup> in an argon atmosphere

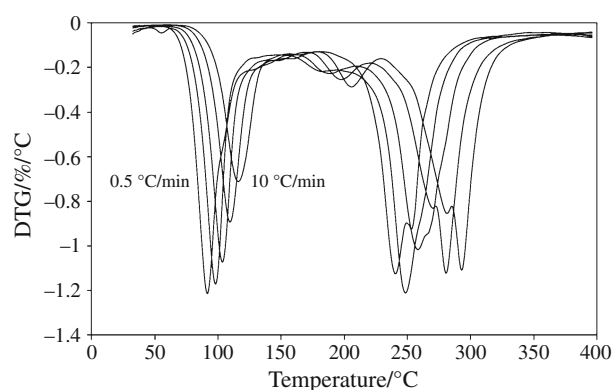


**Fig. 3** TG-DTG plot of DMU in air at heating rates of 0.5, 1, 2, 5 and 10 °C min<sup>-1</sup>

mechanistic approach to the kinetic analysis of the polycondensation of DMU by non-isothermal methods is inhibited by the limitation that a single process cannot be easily identified. To overcome this issue the induction period method was selected allowing the determination of the storage life of the DMU. The induction period method is a model free approach that states that the process can be described by two general mechanistic steps [8, 9, 12]; the induction period during which time no apparent chemical change is taking place and the process itself where, for DMU, the polycondensation takes place. A measure of the stability of the monomer prior to polycondensation can be ascribed to the length of the induction period at any particular temperature.

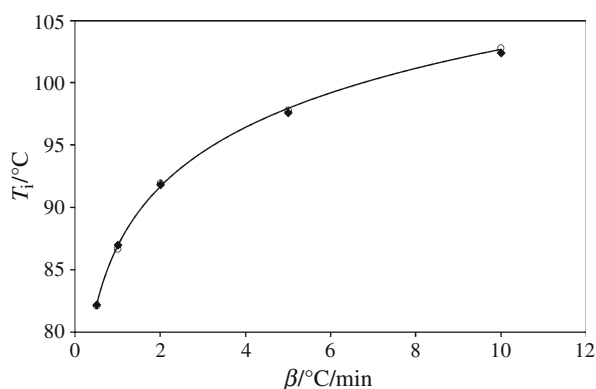
Equations 1, 3 and 4 were used for the determination of the kinetic parameters using onset temperatures of polycondensation in the non-isothermal TG data shown in Fig. 3. The onset of polycondensation is assumed to be the temperature at which the induction period ends. Values of the fitting parameters determined are listed in Table 1. The values of the estimated onset temperatures,

**Table 1** List of fitted parameters to Eqs. 1, 3 and 4 and calculated lengths of the induction periods for isothermal polycondensation at laboratory temperature (23 °C) and refrigerator temperature (4 °C)

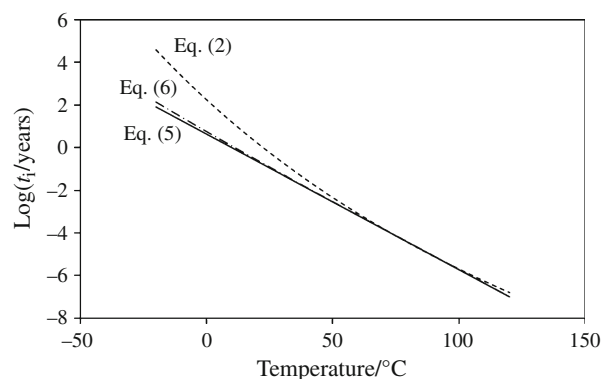
Equation	Eq.	Parameter 1	Parameter 2	$t_i$ (23 °C)/year	$t_i$ (4 °C)/year
$\beta = \int_0^{T_i} \frac{dT}{A \exp(B/T)}$	1	$A = (4.1 \pm 3.7) \times 10^{-23} \text{ min}$	$B = (19230 \pm 320) \text{ K}$	1.3	111
$T_i = \frac{1}{\beta} \ln(CD\beta + 1)$	3	$C = (4.8 \pm 2.0) \times 10^{23} \text{ min}$	$D = (0.146 \pm 0.001) \text{ K}^{-1}$	0.15	2.4
$T_i = T_\infty(1 - \exp(-\beta^a))$	4	$T_\infty = (569.5 \pm 0.1) \text{ K}$	$a = 0.03269 \pm 0.0003$	0.16	3.0

**Table 2** Measured and calculated values of the onset temperatures determined using Eqs. 1, 3 and 4

$\beta/$ °C min <sup>-1</sup>	$T_i$ —Measured/ °C	$T_i$ —Eq. 1/ °C	$T_i$ —Eq. 2/ °C	$T_i$ —Eq. 3/ °C
0.5	82.2	82.5	82.2	82.2
1	87.0	86.9	87.0	87.0
2	91.8	91.5	91.7	91.7
5	97.6	97.7	98.0	98.0
10	102.4	102.5	102.7	102.7

**Fig. 4** Plot of the onset temperature data fitted with Eqs. 3 and 4 using the values of the fitting parameters listed in Table 1. Both fits overlap so that only one curve is apparently visible. Data points shown are the measured data (diamond) and data calculated using Eq. 1 (circle)

$T_i$  are listed in Table 2. The experimental values of  $T_i$  are plotted in Fig. 4 along with the values calculated using Eq. 1 and the curves determined from Eqs. 3 and 4. All of these functions fit the data closely in the experimental temperature range. The values of the kinetic parameters were then used in Eqs. 2, 5 and 6 for the estimation of the length of the induction period under isothermal conditions. Estimates of the length of the induction period, and, hence, storage life, at laboratory (23 °C) and refrigerator temperatures (4 °C) are also listed in Table 1. The estimates of the length of the induction period vary significantly, particularly for those values determined using Eq. 2 at 4 °C. Experience suggests that DMU is viable at

**Fig. 5** Plot of isothermal induction periods calculated from Eqs. 2, 5 and 6 using the fitting parameters listed in Table 1

storage periods of up to 1 year which is more in accordance with the estimates determined using the non-Arrhenian temperature functions.

To exemplify the effect of extrapolation, values of the logarithm of the induction period calculated using Eqs. 2, 4 and 5 for isothermal polycondensation in the range  $-20$  to  $120$  °C are plotted in Fig. 5. Prediction of the induction period for all three models corresponds well in the experimental temperature range of  $82$ – $102$  °C. However, extrapolation beyond the experimental temperature range results in significant deviation for the three functions used. As experience suggests that storage times of the order of a year are the maximum for the DMU synthesised for this study, the deviation through extrapolation outside the experimental temperature range is greatest for the kinetic model using the Arrhenius temperature function and, hence, the non-Arrhenian temperature functions are considered to best represent the kinetic modelling for the case of the onset of polycondensation in DMU. It is, however, important to note that each of the functions applied to the kinetic modelling are approximations based on the single step assumption. These constitutive equations are, therefore, empirical in nature and do not reflect any ongoing mechanistic processes. Hence, use of these functions in lifetime estimation must be made with reference to experience or with awareness that error in estimation increases with increasing degree of extrapolation.

## Conclusions

The polycondensation of DMU was confirmed to occur through the elimination of water and formaldehyde. As these products were produced simultaneously in the TG-MS, the unstable methylene-ether bridges are rapidly decomposed by the elimination of formaldehyde to produce the methylene bridges.

Modelling of the kinetics to estimate the length of the induction period resulted in significant deviation of the estimated induction periods between the models used. The deviation was observed to increase significantly with increasing extrapolation from the experimentally measured data. Experience suggested that the non-Arrhenian temperature functions produced the best estimates of the induction periods for the polycondensation and, hence, the best estimates of the storage life for DMU.

## References

1. Steele R, Giddings LE. Reaction of cellulose with dimethylol- and monomethylolureas. *Ind Eng Chem*. 1956;48:110–4.
2. Pfuhler S, Wolf HU. Effects of the formaldehyde releasing preservatives dimethylol urea and diazolidinyl urea in several short-term genotoxicity tests. *Mutat Res*. 2002;514:133–46.
3. Marvel CS, Elliott JR, Boettner FE, Yuska H. The structure of urea-formaldehyde resins. *J Am Chem Soc*. 1946;68:1681–6.
4. Minopoulou E, Dessiprib E, Chryssikosc GD, Gionisc V, Paipetisc A, Panayiotou C. Use of NIR for structural characterization of urea-formaldehyde resins. *Int J Adhes Adhes*. 2003;23:473–84.
5. Hodgins TS, Hovey AG. Urea-formaldehyde film forming compositions. *Ind. Eng.Chem*. 1939;31:673–8.
6. Christjanson P, Siimer K, Pehk T, Lasn I. Structural changes in urea-formaldehyde resins during storage. *Eur J Wood Wood Prod*. 2002;60:379–84.
7. Langmaier F, Šivarová J, Mládek M, Kolomazník K. Curing adhesives of urea-formaldehyde type with collagen hydrolysates of chrome-tanned leather waste. *J Therm Anal Calorim*. 2004; 75:205–19.
8. Šimon P, Kučma A. DSC analysis of the induction period in the vulcanisation of rubber compounds. *J Therm Anal Calorim*. 1999;56:1107–13.
9. Šimon P. Material stability predictions applying a new non-Arrhenian temperature function. *J Therm Anal Calorim*. 2009;97(2): 391–6.
10. Bishop DW, Thomas PS, Ray AS, Šimon P. Two-stage kinetic model for the  $\alpha$ - $\beta$  phase recrystallisation in nickel sulphide. *J Therm Anal Calorim*. 2001;64:201–10.
11. Šimon P. The Single-step approximation: strong and weak sides. *J Therm Anal Calorim*. 2007;88(3):709–15.
12. Šimon P, Hynek D, Malíková M, Cibulková Z. Extrapolation of accelerated thermooxidative tests to lower temperatures applying non-arrhenius temperature functions. *J Therm Anal Calorim*. 2008;93(3):817–21.
13. D'Alelio GF. *Experimental Plastics and Synthetic Resins*. New York: Wiley; 1955.
14. Kumlin K, Simonson R. Urea-formaldehyde resins. Part 2. The formation of N, N-dimethylolurea and trimethylolurea in urea-formaldehyde mixtures. *Angew Makromolek Chem*. 1978; 72(1):67–74.